NASA TN D-369

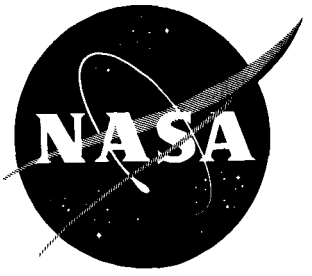

TECHNICAL NOTE

D-369

INVESTIGATION OF THE LOW-SUBSONIC FLIGHT CHARACTERISTICS OF A MODEL OF AN ALL-WING HYPERSONIC BOOST-GLIDE CONFIGURATION HAVING VERY HIGH SWEEP

By Robert E. Shanks

Langley Research Center
Langley Field, Va.

NATIONAL AERONAUTICS AND SPACE ADMINISTRATION

WASHINGTON June 1960

NATIONAL AERONAUTICS AND SPACE ADMINISTRATION

TECHNICAL NOTE D-369

INVESTIGATION OF THE LOW-SUBSONIC FLIGHT CHARACTERISTICS OF A MODEL OF AN ALL-WING HYPERSONIC BOOST-GLIDE CONFIGURATION HAVING VERY HIGH SWEEP

By Robert E. Shanks

SUMMARY

An investigation of the low-subsonic flight characteristics of a model of an all-wing hypersonic boost-glide configuration has been made in the Langley full-scale tunnel over an angle-of-attack range from about 15° to 30°. Static force tests were made in the Langley free-flight tunnel over an angle-of-attack range from 0° to 32°.

The longitudinal stability and control characteristics were considered satisfactory when the model had positive static longitudinal stability. It was possible to fly the model with a small amount of static instability but the longitudinal characteristics were considered unsatisfactory in this condition. The lateral stability and control characteristics were considered to be poor through the flight-test angle-of-attack range because of weak control response and because the model had a Dutch roll oscillation that was only lightly damped at an angle of attack of 15°, neutrally stable at an angle of attack of 20°, and unstable at angles of attack of 25° and above. Artificial damping in roll greatly improved the lateral characteristics and resulted in flights being made at angles of attack of up to 30°.

INTRODUCTION

An investigation is being conducted by the National Aeronautics and Space Administration to provide information on the stability and control characteristics of some proposed hypersonic boost-glide configurations over the speed range from hypersonic to low-subsonic speeds. The present investigation was made to provide some information at low-subsonic speeds on the longitudinal and lateral stability and control characteristics of a model of an all-wing hypersonic-glider configuration having a leading-edge sweep of about 80°.

The investigation included flight tests in the Langley full-scale tunnel to determine the low-subsonic flight characteristics of the model over an angle-of-attack range from about 15° to 30°, and force tests in the Langley free-flight tunnel to determine the static stability and control characteristics over an angle-of-attack range from 0° to 32°.

Included in the flight-test investigation was a study to determine the effect of center-of-gravity location on the longitudinal stability and control characteristics of the model at an angle of attack of about 20°. Also studied in the flight tests was the effect of artificial roll damping on the lateral stability and control characteristics.

SYMBOLS

The longitudinal forces and moments were determined with respect to the wind axes and the lateral forces and moments were determined with respect to the body axes. (See fig. 1.) The axes originated at a center-of-gravity position located at 35 percent mean aerodynamic chord. All measurements are reduced to standard coefficient form and presented in terms of the following symbols:

b wing span, ft

C_D drag coefficient, $\frac{F_D}{qS}$

C_L lift coefficient, $\frac{F_L}{qS}$

C_Y side-force coefficient, $\frac{F_Y}{qS}$

$C_{Y_\beta} = \frac{\partial C_Y}{\partial \beta}$ per deg

C_l rolling-moment coefficient, $\frac{M_X}{qSb}$

$C_{l_\beta} = \frac{\partial C_l}{\partial \beta}$ per deg

C_m pitching-moment coefficient, $\frac{M_Y}{qS\bar{c}}$

C_n	yawing-moment coefficient, $\frac{M_Z}{qSb}$
$C_{n_p} = \frac{\partial C_n}{\partial \frac{pb}{2V}}$	per radian
$C_{n_\beta} = \frac{\partial C_n}{\partial \beta}$	per deg
$\bar{c}$	wing mean aerodynamic chord, ft
F_D	drag force, lb
F_L	lift force, lb
F_Y	side force, lb
I_X	moment of inertia about X-axis, slug-ft^2
I_Y	moment of inertia about Y-axis, slug-ft^2
I_Z	moment of inertia about Z-axis, slug-ft^2
M_X	rolling moment, ft-lb
M_Y	pitching moment, ft-lb
M_Z	yawing moment, ft-lb
p	rolling velocity, radians/sec
q	dynamic pressure, $\frac{\rho V^2}{2}$, lb/sq ft
S	wing area, sq ft
V	airspeed, ft/sec
X,Y,Z	longitudinal, lateral, and vertical body axes
α	angle of attack, deg
β	angle of sideslip, deg

δ_a aileron deflection, deg

δ_e elevator deflection (positive down), deg

δ_r rudder deflection (negative to right), deg

ρ air density, slugs/cu ft

APPARATUS AND TESTING TECHNIQUE

Model

The model used in the investigation was constructed at the Langley Research Center and was assumed to be a 1/10-scale model of a possible hypersonic boost-glide configuration. A three-view drawing of the model is shown in figure 2, and photographs of the model are shown as figure 3. Table I gives the dimensional and mass characteristics of the model. Elevons consisting of plain flaps extending rearward from the trailing edge of the bottom surface of the wing were used for elevator and aileron control, and outward deflecting surfaces located at the wing tips were used for rudder controls. Two rudder surfaces differing in size were used in the investigation (fig. 2): the original rudder which had most of its area above the model center line and a modified rudder which had about twice the area of the original rudder with most of the additional area below the center line.

For the flight tests, thrust was provided by compressed air supplied through flexible hoses to two nozzles at the rear of the fuselage. The amount of thrust could be varied and the maximum output per nozzle was about 10 to 12 pounds. The controls were operated remotely by pilots by means of flicker (full on or off) pnuematic servomechanisms which were actuated by electric solenoids. Artificial stabilization in roll was provided by a simple rate damper. An air-driven rate gyroscope was the sensing element and the signal was fed into a servoactuator which deflected the elevons in proportion to rolling velocity. The manual control was superimposed on the control deflection resulting from the rate signal.

Test Equipment and Setup

The static force tests were conducted in the Langley free-flight tunnel. The model was sting mounted, and the forces and moments were measured about the body axes by using internal strain-gage balances.

The flight investigation was conducted in the Langley full-scale tunnel with the test setup illustrated in figure 4. The model is remotely controlled by a roll-yaw pilot, a pitch pilot, and a thrust controller. Compressed air for thrust and electric power for the control actuators are supplied through a slack overhead line which also acts as a safety cable to prevent the model from crashing when it goes out of control. A more complete description of the test technique used in making free-flying model tests is given in reference 1.

STABILITY AND CONTROL PARAMETERS OF FLIGHT-TEST MODEL

Force tests were made to determine the static longitudinal and lateral stability and control characteristics of the model. The tests were made at a dynamic pressure of 4.5 pounds per square foot which corresponds to an airspeed of about 61 feet per second at standard sea-level conditions and to a test Reynolds number of 2,150,000 based on the mean aerodynamic chord of 5.48 feet.

Static Longitudinal Stability and Control

The static longitudinal stability and control tests were made for an angle-of-attack range from 0° to 32° for elevator settings from -20° to 30° in 10° increments. The effect of elevator deflection on the longitudinal characteristics of the model is shown in figure 5. These data show that the longitudinal stability of the model was fairly constant over most of the angle-of-attack range and then decreased rather abruptly and became unstable at the highest angles. These data also show that the elevator effectiveness varied considerably with angle of attack and with positive or negative deflection, apparently because of a shielding effect experienced by this type of elevon behind the blunt body.

Static Lateral Stability and Control

The static lateral stability tests were made over a range of sideslip angles from 20° to -20° for angles of attack from 0° to 32°. The data are presented as the variation of the coefficients C_Y, C_n, and C_l with angle of sideslip for various angles of attack in figures 6 and 7 for the original and modified rudders, respectively. These data are summarized in figure 8 as the variations with angle of attack of the side-force parameter C_{Y_β}, the directional-stability parameter C_{n_β}, and the effective-dihedral parameter $-C_{l_\beta}$, which were obtained by

measuring the slopes of the curves at angles of sideslip between -5° and 5°. The data of figure 8 show that the model had positive directional stability over the angle-of-attack range and that the modified rudders provided a positive increment of directional stability at all angles of attack. The data also show that the model had positive effective dihedral over the angle-of-attack range and that the modified rudders had little effect on the values of $-C_{l_\beta}$ over most of the angle-of-attack range.

The aileron control effectiveness of the model with the original and with the modified rudders is shown in figure 9. These data show that the rolling moments produced by the original ailerons were generally constant over the angle-of-attack range and were little affected by the rudder configurations studied. The magnitude of the adverse yawing moments, however, was considerably smaller with the modified rudders than with the original rudders.

The control effectiveness of the original and modified rudders is shown in figure 10. The data show that the rudders produced favorable yawing moments over the angle-of-attack range and that the modified rudder greatly increased the yawing moment available.

In flight, the rudders and ailerons were usually operated simultaneously and the resulting yawing moments produced by combined aileron and rudder deflection are compared in figure 11 for the original and modified rudders. Deflection of the ailerons (±10°) and original rudders (±15°) produced large adverse yawing moments over the angle-of-attack range, whereas the ailerons and modified rudders produced small to fairly large favorable yawing moments.

FLIGHT TESTS

Flight tests were made to determine the dynamic stability and control characteristics of the model over an angle-of-attack range from about 15° to 30°. The model was tested with the original rudders and with the modified rudders. Flights were made at an angle of attack of 20° to determine the effect of center-of-gravity position on the longitudinal characteristics of the model. Flights were also made over the angle-of-attack range to determine the effect of artificial roll damping on the lateral stability and control characteristics.

Flights were made with coordinated aileron and rudder control and also with ailerons alone. The control deflections used for most of the flight tests were $\delta_a = \pm 10°$, $\delta_e = \pm 15°$, and $\delta_r = \pm 15°$.

The model behavior during flight was observed by the pitch pilot located at the side of the test section and by the roll and yaw pilot located in the rear of the test section. The results obtained in the flight tests were primarily in the form of qualitative ratings of flight behavior based on pilot opinion. The motion-picture records obtained in the tests were used to verify and correlate the ratings for the different flight conditions.

FLIGHT-TEST RESULTS AND DISCUSSION

A motion-picture film supplement covering flight tests of the model has been prepared and is available on loan. A request card form and a description of the film will be found at the back of this paper, on the page immediately preceding the abstract and index page.

Longitudinal Stability and Control

During the investigation made to study the longitudinal stability and control characteristics of the model, artificial damping in roll was used in order to minimize any effects lateral motions might have on the longitudinal behavior.

As part of the longitudinal investigation a series of flights were made at 20° angle of attack to determine the effect of center-of-gravity location. Static tests indicated that at this angle of attack the model was neutrally stable at a center-of-gravity position of about 39 percent of the mean aerodynamic chord. With positive stability (center of gravity ahead of the 39-percent mean-aerodynamic-chord location) the model was easy to fly and the pilot had no trouble controlling it. With neutral stability, the model was somewhat more difficult to fly in that it required more attention on the part of the pilot to keep it flying smoothly. With the center of gravity at 41 percent of the mean aerodynamic chord, the model reacted rather sharply to gusts and control disturbances and the pilot had to pay very close attention to the elevator control in order to recover from disturbances. Although this was the most rearward center-of-gravity location at which flights were attempted, it was felt that sustained flights would have been possible with the center of gravity 1 or 2 percent farther rearward with the elevator control used ($\delta_e = \pm 15^\circ$). Results of the tests of reference 1 and the analog studies of reference 2 showed that the use of artificial damping in pitch would afford a definite improvement in the longitudinal characteristics for statically unstable conditions.

In addition to the center-of-gravity range studies made at an angle of attack of 20°, flights were made at angles of attack from 15° to 30°

with a center-of-gravity location (35 percent $\bar{c}$) that gave good static longitudinal stability at an angle of attack of 20°. The longitudinal characteristics of the model were generally satisfactory for angles of attack up to about 25°. Above 25° a mild pitchup tendency was noted and careful attention to elevator control was required to prevent the model from nosing up and diverging in pitch.

Lateral Stability and Control

Preliminary tests indicated that sustained flights of the model were impossible with the original rudders. Therefore, all results discussed herein are for the model with the modified rudders.

No roll damping added.- The lateral stability and control characteristics of the model were considered to be poor throughout the flight-test angle-of-attack range. At an angle of attack of about 15° the Dutch roll oscillation was lightly damped. Because of the large ratios of I_Z/I_X and C_{l_β}/C_{n_β} for this model the oscillation appeared to be an almost pure rolling motion about the body axis. It was difficult to fly the model smoothly not only because of the low damping of the Dutch roll oscillation but also because of low control effectiveness which made it necessary for the pilot to pay close attention to control. Even though the rudder size had been increased the pilot felt that still greater rudder yawing moments were necessary to improve the control characteristics. The data of figure 11 show that in the angle-of-attack range of the flight tests (15° to 30°) only small favorable yawing moments were produced by combined aileron and rudder control. It was usually impossible to recover the model from large disturbances because of the generally poor control characteristics.

As the angle of attack increased, the Dutch roll oscillation became less damped, and at about 20° angle of attack the model had a constant-amplitude oscillation. The lateral control was not effective in stopping the oscillation, but it was possible to move the model around in the test section or hold one position fairly well by paying close attention to controls. As the angle of attack increased to about 25° the oscillation became unstable and the model went out of control despite the efforts of the pilot to control it.

Roll damping added.- The addition of rate roll damping to improve the stability of the Dutch roll oscillation greatly improved the lateral characteristics of the model so that flights could be made up to about maximum lift (α = 30°) where the model diverged in sideslip. While the rate damper increased the damping in roll it also introduced large positive values of C_{n_p} (because of the large yawing moments produced by the

elevons) which probably made the behavior of the model somewhat more erratic than it would have been if only pure damping in roll had been added. Use of the roll damper resulted in a decrease in response of the model to roll control, but did not have any appreciable effect on the ability of the pilot to control the model.

CONCLUSIONS

The results of the investigation can be summarized as follows:

1. The longitudinal stability and control characteristics of the model were satisfactory when the model had positive static longitudinal stability. It was possible to fly the model with a small amount of static instability but the longitudinal characteristics were considered unsatisfactory in this condition.

2. The lateral stability and control characteristics were considered to be poor throughout the flight-test angle-of-attack range because of weak control response and because the model had a Dutch roll oscillation that was only lightly damped at an angle of attack of 15°, neutrally stable at an angle of attack of 20°, and unstable at angles of attack of 25° and above. Artificial damping in roll greatly improved the lateral characteristics and resulted in flights being made up to 30° angle of attack.

Langley Research Center,
National Aeronautics and Space Administration,
Langley Field, Va., January 26, 1960.

REFERENCES

1. Paulson, John W., and Shanks, Robert E.: Investigation of Low-Subsonic Flight Characteristics of a Model of a Flat-Bottom Hypersonic Boost-Glide Configuration Having a 78° Delta Wing. NASA TM X-201, 1959.

2. Moul, Martin T., and Brown, Lawrence W.: Effect of Artificial Pitch Damping on the Longitudinal and Rolling Stability of Aircraft With Negative Static Margins. NASA MEMO 5-5-59L, 1959.

TABLE I

GEOMETRIC AND MASS CHARACTERISTICS OF THE TEST MODEL

Gross weight, lb	34.2
I_X, slug-ft^2	0.20
I_Y, slug-ft^2	2.04
I_Z, slug-ft^2	2.62

Wing:

Airfoil section	6° wedge
Area, sq ft	12.1
Span, ft	2.5
Aspect ratio	0.52
Root chord, ft	7.5
Tip chord, ft	1.5
Mean aerodynamic chord, ft	5.48
Sweep, leading edge, deg	72.6, 79.9, and 90
Dihedral, lower surface, deg	16.4
Dihedral, upper surface, deg	-16.4
Leading-edge diameter, ft	0.01

	Original	Modified
Vertical tails (each):		
Airfoil section	Flat plate	Flat plate
Height, ft	0.32	0.58
Aspect ratio	0.33	0.72
Area:	0.30	0.47
Rudder, sq ft	0.14	0.31
Fin, sq ft	0.16	0.16
Root chord, ft	1.50	1.54
Tip chord, ft	0.50	0.54
Sweep of leading edge, deg	75	75

Elevons (each):

Airfoil section	Flat plate
Taper ratio	1.0
Area, sq ft	0.65

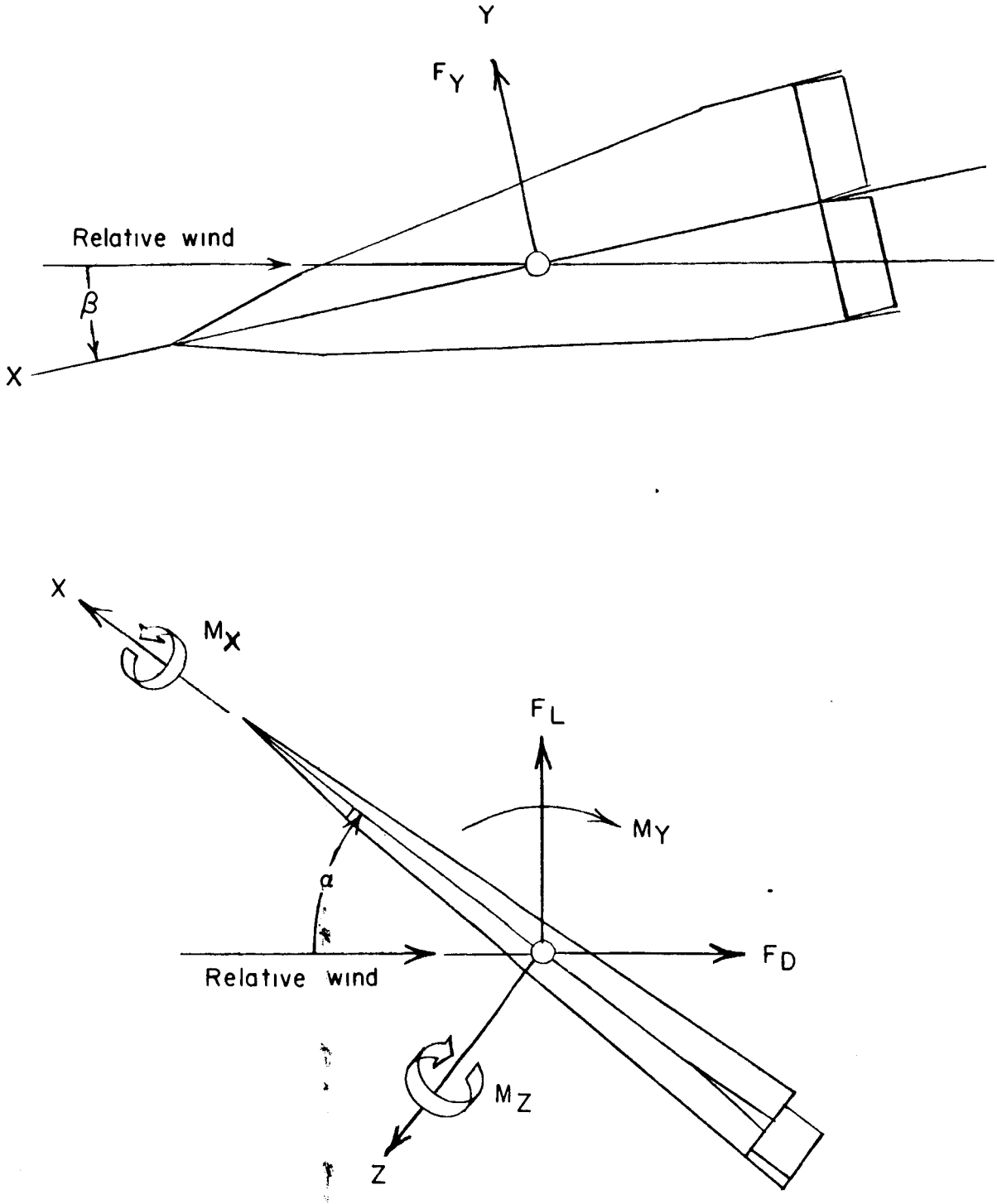

Figure 1.- Sketch of body-axis system showing positive direction of forces, moments, and angles.

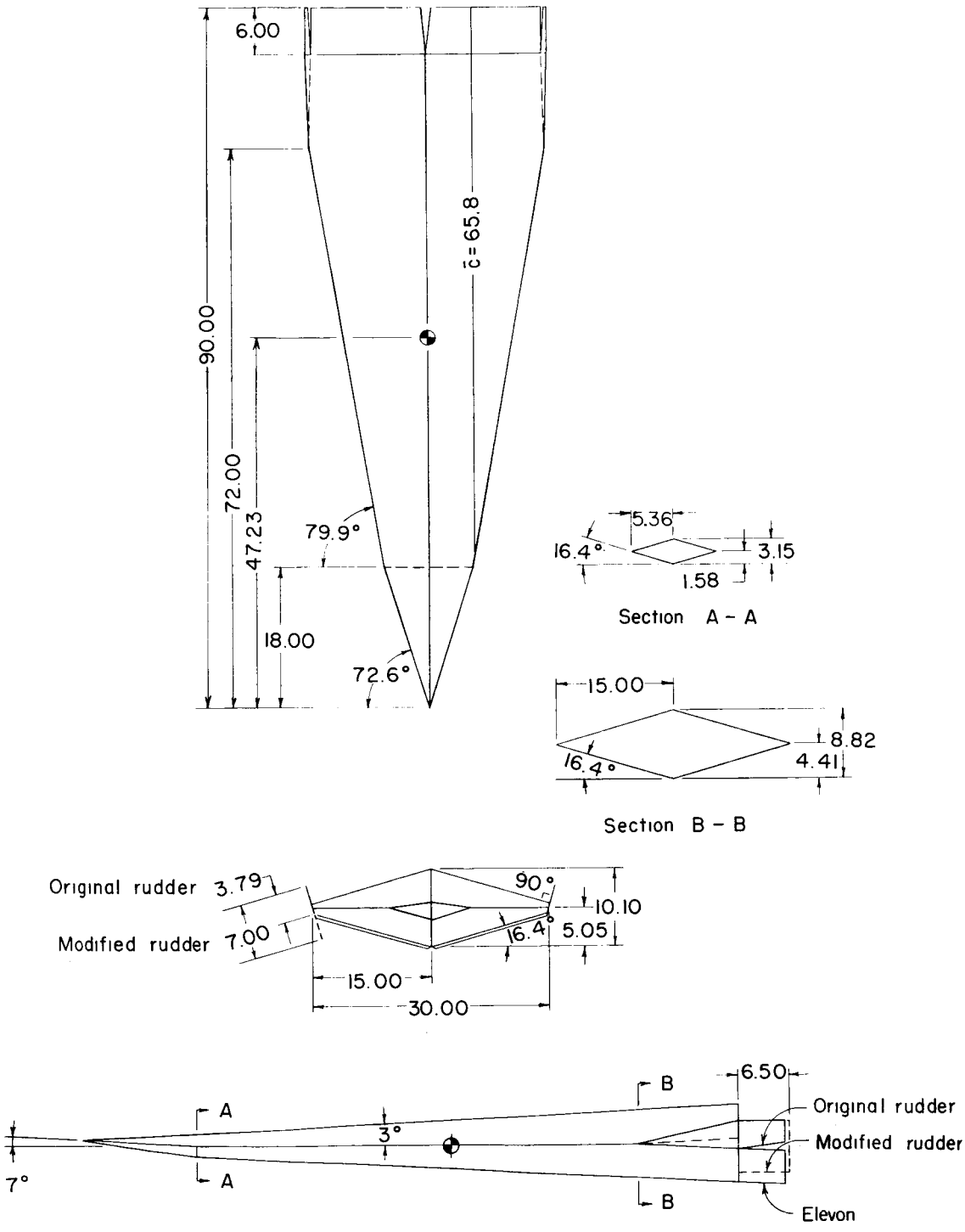

Figure 2.- Three-view drawing of model used in investigation. All dimensions are in inches.

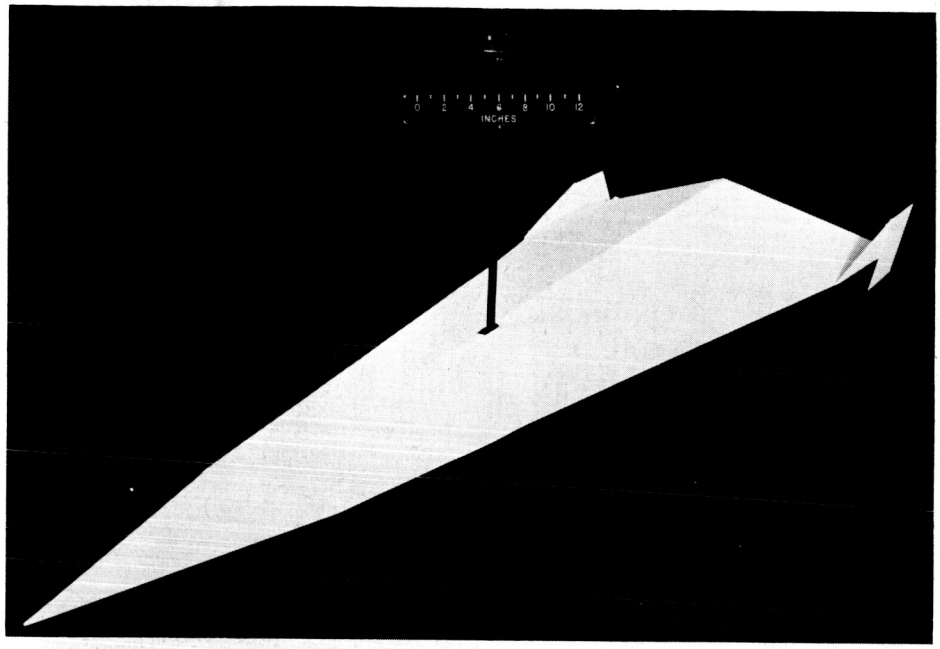

L-57-4846

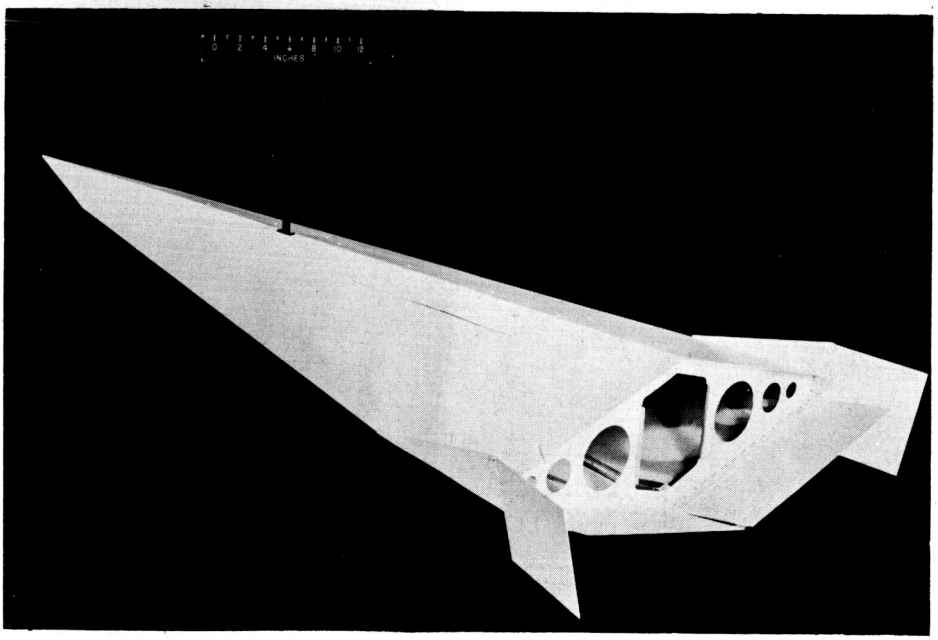

L-57-4849

Figure 3.- Photographs of the test model as used in the static force tests. Modified rudder configuration.

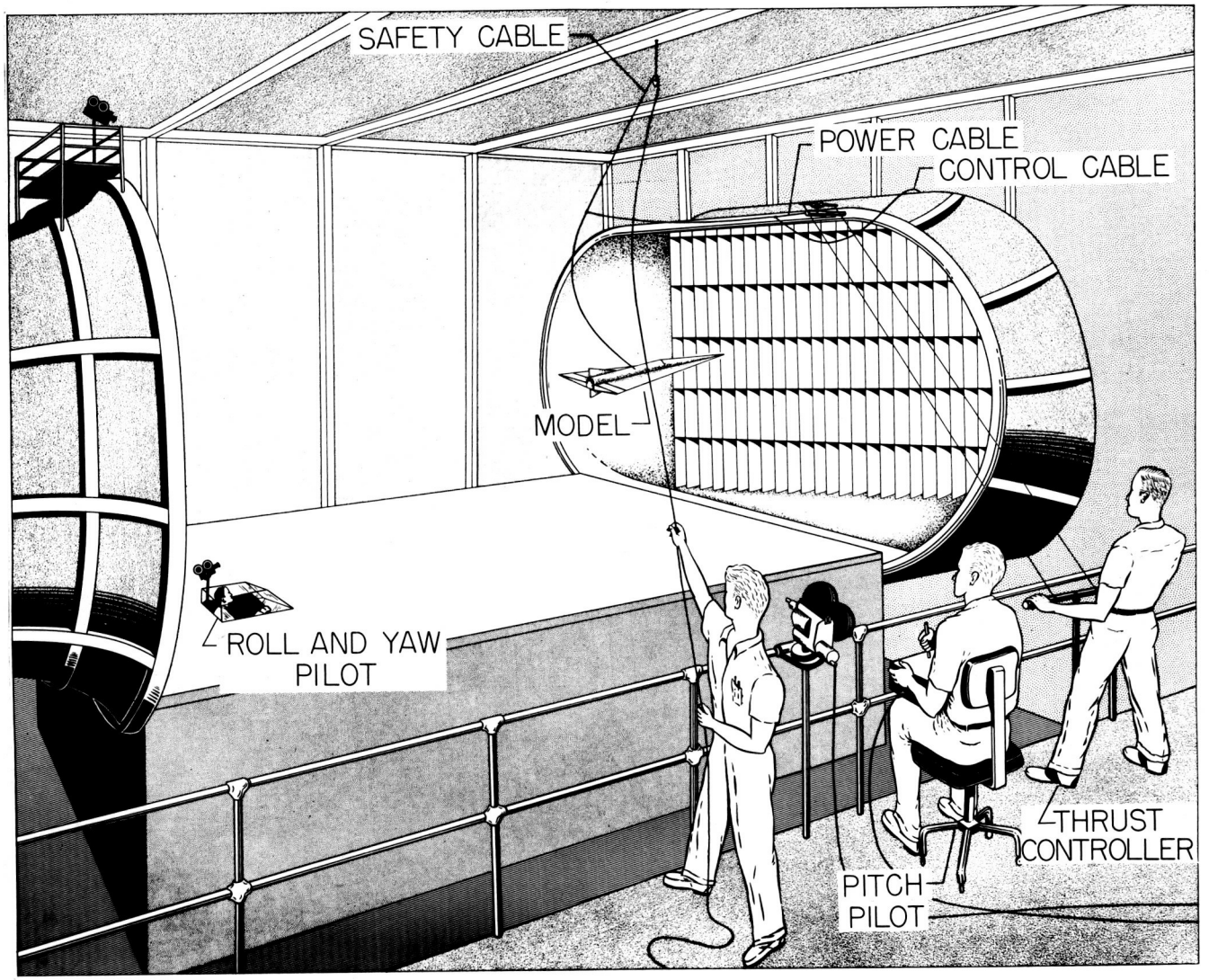

Figure 4.- Flight-test setup in the Langley full-scale tunnel.

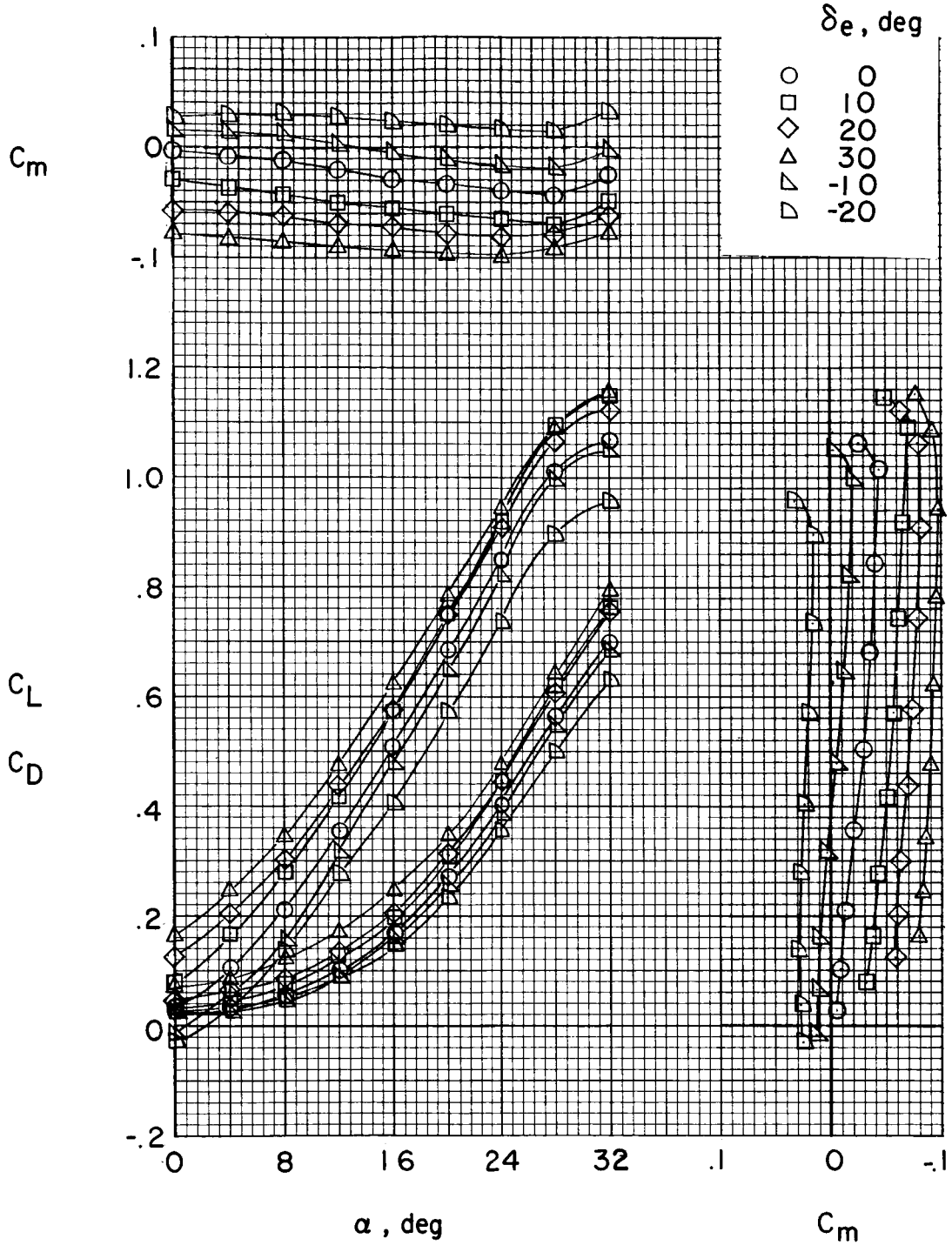

Figure 5.- Effect of elevator deflection on longitudinal characteristics of model. Modified rudders; $\beta = 0^{\circ}$.

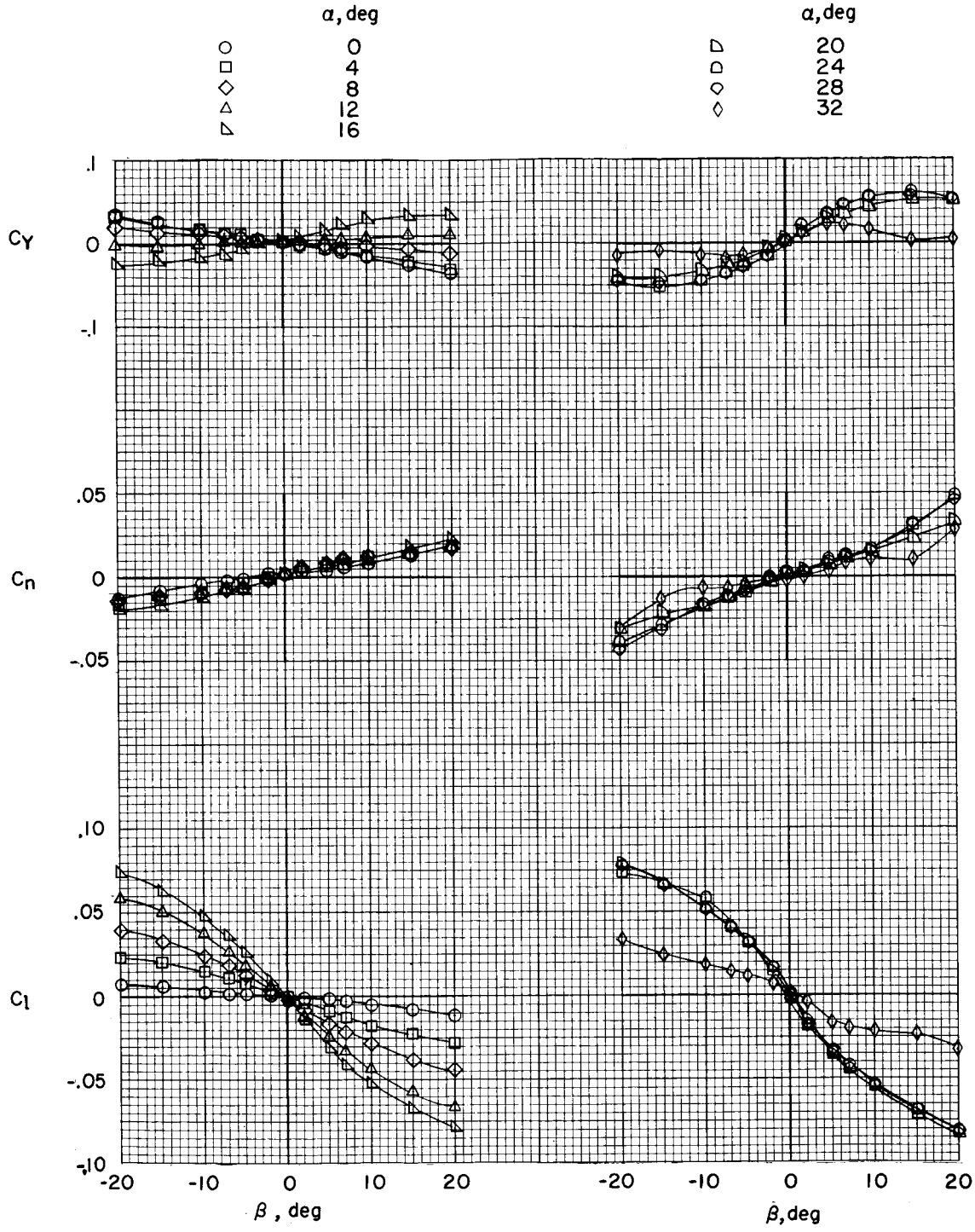

Figure 6.- Variation of static lateral coefficients with angle of sideslip. Original rudders; $\delta_e = 0^\circ$.

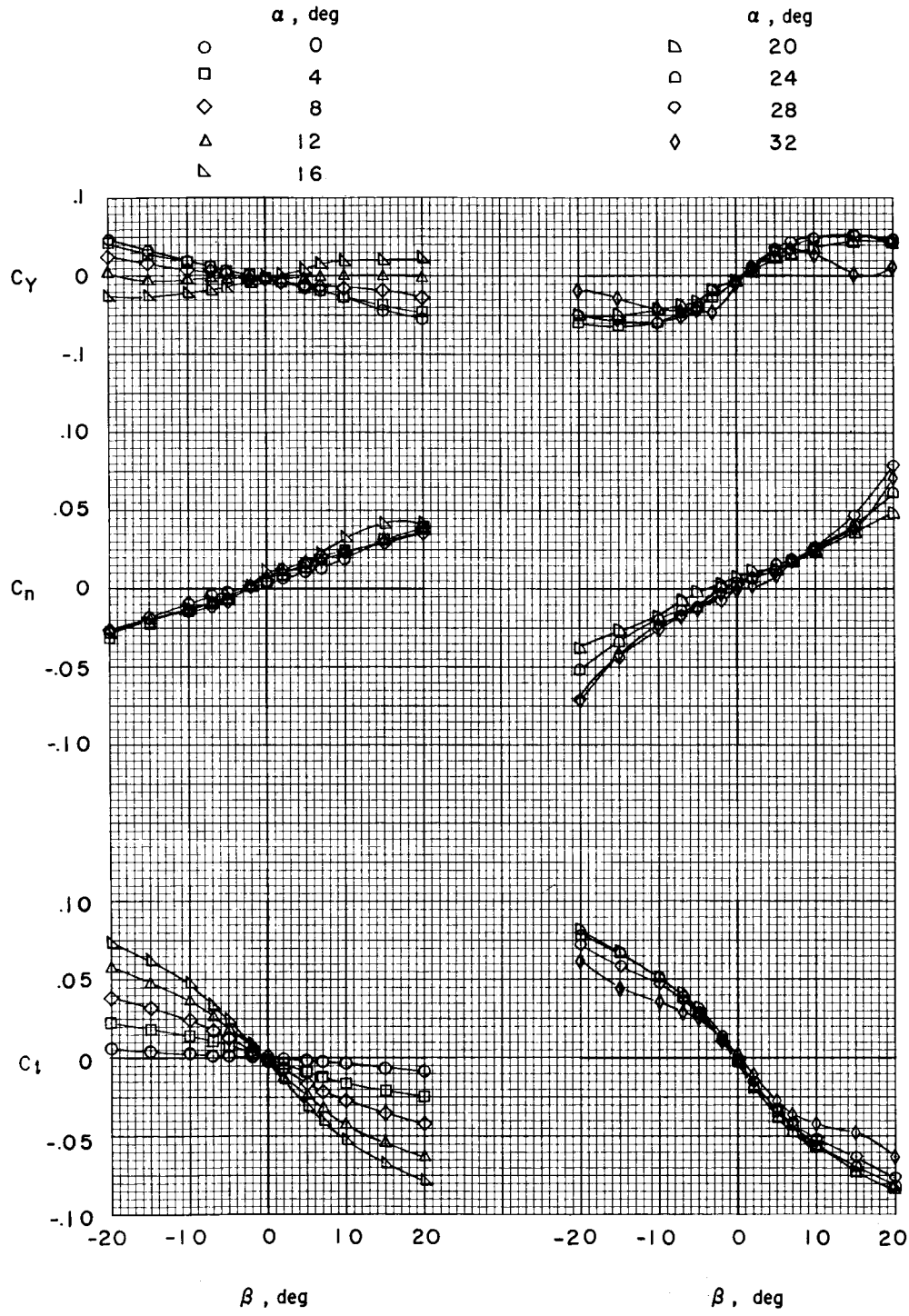

Figure 7.- Variation of static lateral coefficients with angle of sideslip. Modified rudders; $\delta_e = 10^\circ$.

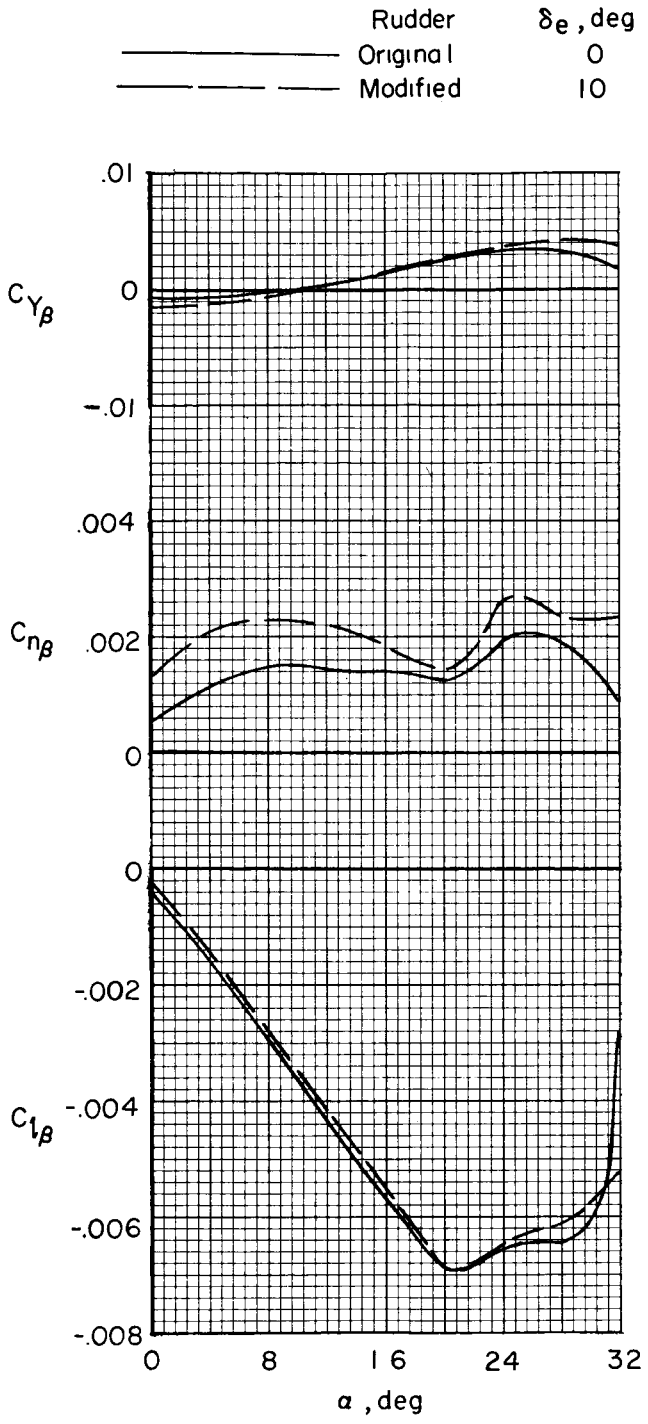

Figure 8.- Variation of the static lateral stability derivatives with angle of attack; $\beta = -5^\circ$ to 5°.

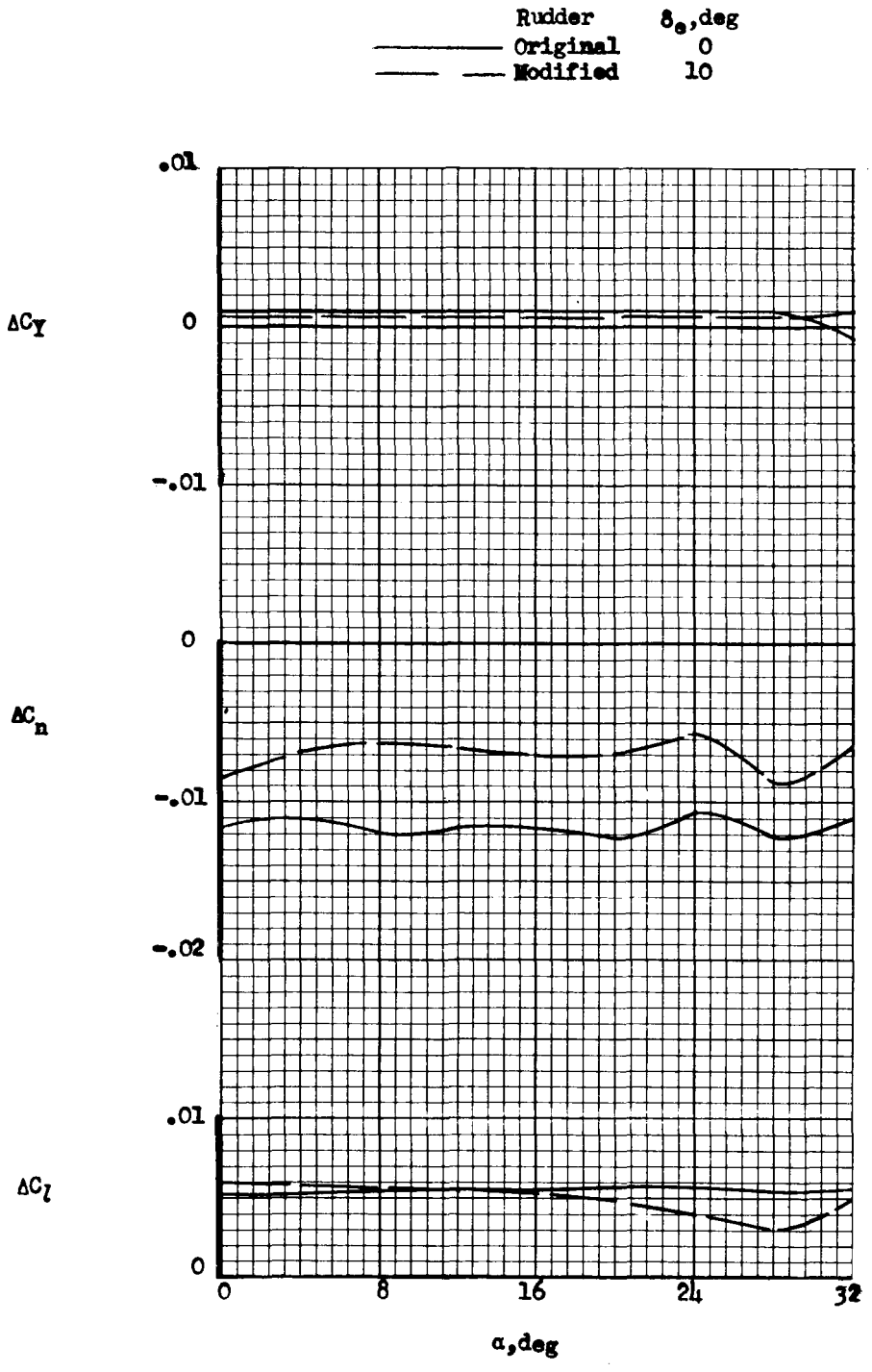

Figure 9.- Incremental lateral control coefficients due to aileron deflection of 10° down on left elevon and 10° up on right elevon; $\beta = 0^\circ$.

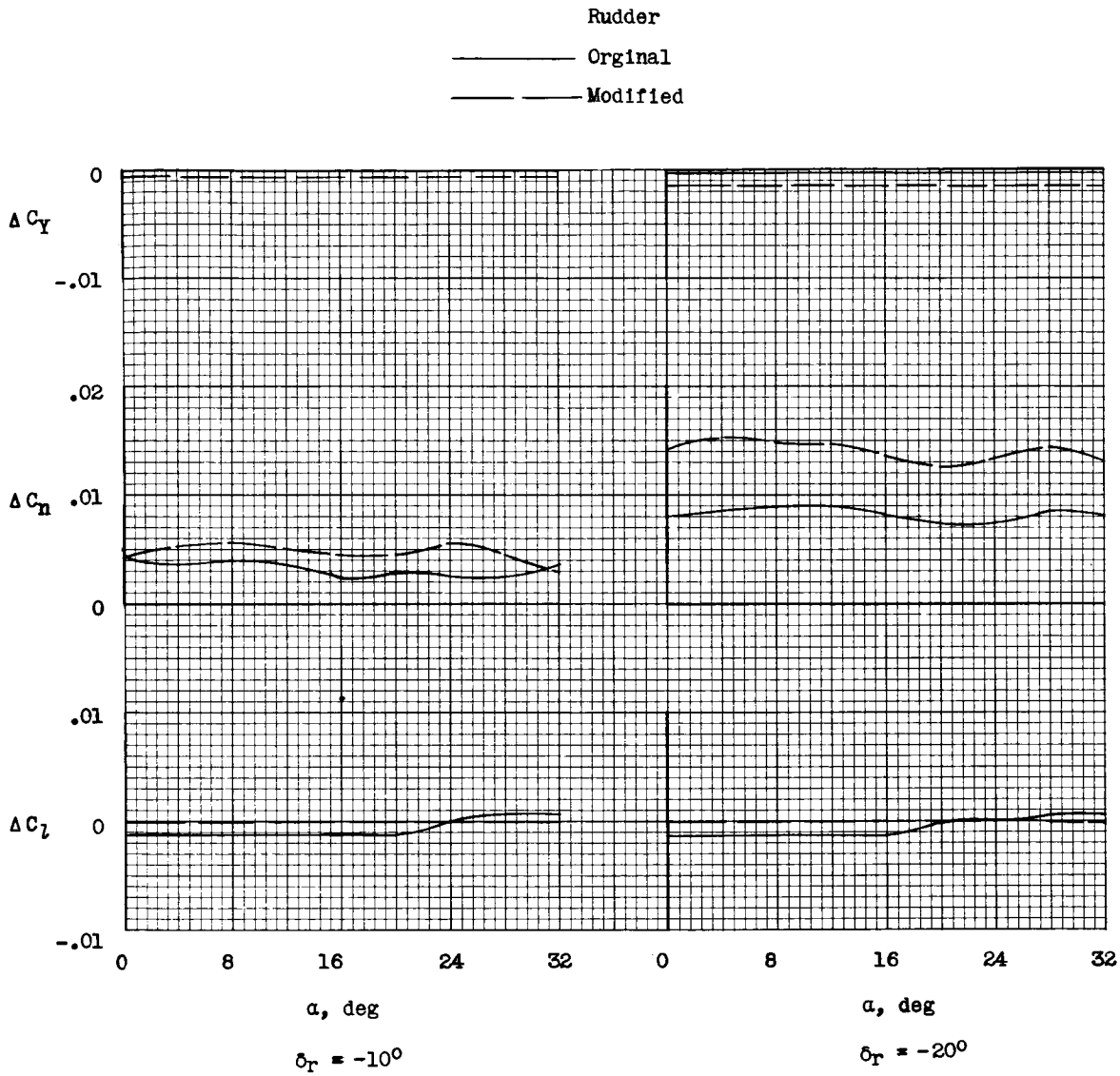

Figure 10.- Incremental lateral control coefficients due to right rudder deflection; $\beta = 0^{\circ}$.

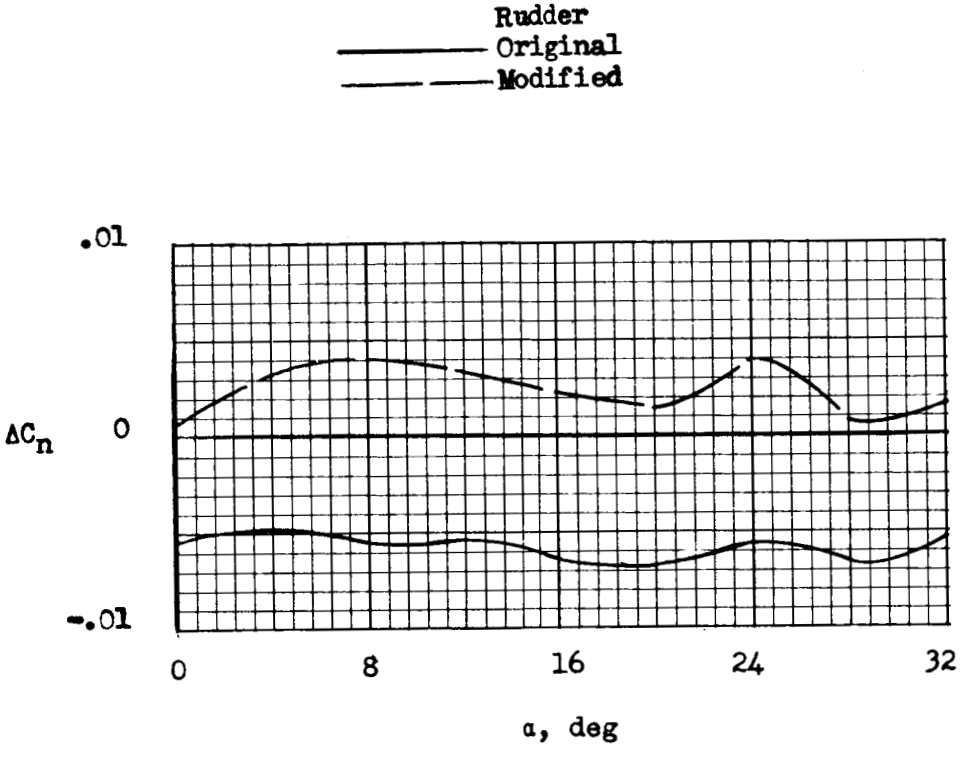

Figure 11.- Net yawing moment due to coordinated rudder and aileron control. $\delta_a = \pm 10^\circ$ (from fig. 9); $\delta_r = -15^\circ$ (estimated from data of fig. 10).